Monday

111-112

THE ENCYCLOPEDIA OF PHYSICS

SECOND EDITION

EDITED BY

Robert M. Besançon
Physical Sciences Administrator
Air Force Materials Laboratory
Wright-Patterson Air Force Base, Ohio

VNR VAN NOSTRAND REINHOLD COMPANY
New York Cincinnati Toronto London Melbourne

TABLE 2. INFRARED DETECTORS

Detector (operating temperature)	Region (μm)	Specific Detectivity, D* at Peak ($cmHz^{1/2}w^{-1}$)	Time Constant (sec)	Special Features
Si(295K)	Visible–1.0	2×10^{12}	5×10^{-6}	Photovoltaic crystal
PbS (295 K)	Visible–2.8	8×10^{10}	2×10^{-4}	Thin-film photoconductor
PbSe (195 K)	Visible–5.6	2×10^{10}	2×10^{-3}	Thin-film photoconductor
InSb (77 K)	1–5.6	10^{11}	$<2 \times 10^{-7}$	Photovoltaic crystal
(Hg · Cd)Te (77 K)	2–14	5×10^{9}	5×10^{-7}	Spectral cut-off varies with alloy composition
Ge (Hg doped) (25 K)	1–16	2×10^{10}	$<10^{-6}$	Photoconductor crystal
Ge (Cu doped (5 K)	1–29	3×10^{10}	$<10^{-6}$	Photoconductor crystal
Ge (Zn doped) (5 K)	1–40	3×10^{10}	10^{-8}	Photoconductor crystal
Thermistor bolometer (295 K)	All	2×10^{8}	10^{-3}–10^{-2}	Flake of mixed oxides
Golay cell (255 K)	All	2×10^{9}	1.5×10^{-2}	Pneumatic
Thermocouple (295 K)	All	2×10^{8}	1.5×10^{-2}	Used in spectrometers

photometer, in which the transmission of monochromatic radiation by a gaseous sample in a cell is compared with that of a blank cell, while the wavelength of the radiation is scanned through the spectral range of interest. Prism dispersing elements are usually used in the infrared, rather than gratings, because of the difficulty with the latter of separating the several orders in the wide spectral range covered. Far infrared spectroscopy is complicated by the omnipresence of background and scattered radiation of shorter wavelength emitted inside the instrument at room temperature. Special techniques of filtering must be employed to eliminate the effects of the short-wavelength radiation.

Optical-electronic devices of many varieties have been designed to determine the direction of weakly radiating remote objects by means of detection of their infrared emission. Military applications have been found which have been made possible uniquely by this technique. Missiles can be guided to their target by infrared detection of the self-emission of heated segments of the target. Detailed maps of the earth's surface can be made from aircraft at night by observing the varying infrared emission of the ground. Personnel can be detected in total darkness by the infrared radiation they emit as warm objects.

Such devices require the detection of low-level radiation in the intermediate infrared region. Optical lenses or mirrors are used to collect the observed radiation and concentrate it onto the sensitive infrared detector. High-gain, low-noise electronic amplifiers must be provided to increase the weak signal from the detector to a level which can be used to operate controls or displays, as demanded by the application. Optical filtering is applied in order to restrict the observed spectral region to one in which the target is effectively detected, with a minimum of interference from radiation from its background. The wavelength of detection is such that angular resolution capability, as set by diffraction, is much greater with infrared devices than that of radar devices. Detection of targets at great distances through intervening atmosphere is more effective in the infrared than in the visible because of the much lower atmospheric scattering in the infrared.

Detailed discussions of the characteristics, detection and applications of infrared radiation may be found in the references.

R. H. MCFEE

References

Jamieson, J. A., McFee, R. H., Plass, G. N., Grube, R. H., and Richards, R. G., "Infrared Physics and Engineering," New York, McGraw-Hill Book Co., 1963.

Smith, R. A., Jones, T. E., and Chasmar, R. P., "The Detection and Measurement of Infrared Radiation," Fair Lawn, N.J., Oxford University Press, 1957.

Herzberg, G., "Infrared and Raman Spectra of Polyatomic Molecules," New York, Van Nostrand Reinhold, 1945.

Szymanski, H. A., and Alperts, N. A., "IR: Theory and Practice of Infrared Spectroscopy," Plenum Press, 1964.

Kruse, P. W., McGlauchlin, L. D., and McQuistan, R. B., "Elements of Infrared Technology," New York, John Wiley & Sons, 1962.

Hudson, R. D., Jr., "Infrared System Engineering," New York, John Wiley & Sons, 1969.

Cross-references: ABSORPTION SPECTRA; LIGHT; RADIATION, THERMAL; SPECTROSCOPY.

INTERFERENCE AND INTERFEROMETRY

Interference is the term used to signify a large class of phenomena in light, and interferometry is the technique of high-precision measurement based on these phenomena. Ordinarily rays of

light crossing the same point in different directions do not interfere with each other; each ray is propagated as though it alone were present. However, there are certain interesting cases when these rays do interfere with each other; the interference may be destructive, as when they cancel each other's effect, or may be constructive, as when they reinforce each other. Interference is a consequence of light being propagated in the form of waves.

Young's Experiment The classic experiment in interference is the one performed by Thomas Young in 1802. A source of light SL (see Fig. 1) that is placed behind a narrow slit illuminates two other slits P and Q which are parallel and very close to each other. At some distance away is a screen which receives the light from the two slits. On the screen is seen a series of bright and dark fringes. If either of the two slits is covered, the fringes disappear, and the screen is almost uniformly illuminated. The combined effect due to the two slits is that at certain points there is no light at all, and at other points the brightness is four times that due to a single slit.

This puzzling phenomenon of light upon light producing darkness can be readily understood by considering the analogous case of ripples on the surface of water. Let a continuous series of ripples be produced by a vibrating metal strip dipping in and out of the surface of water. A light floating body, say a leaflet, wobbles up and down with the same frequency as the vibrator. The ripples spread out in widening circles. If now another vibrator of the same frequency is brought near the first, the appearance of the ripples is completely changed. Along certain radial lines starting from the two vibrators, the water surface seems undisturbed; the leaflet does not move if placed along these lines. In between these lines the ripples have a very large amplitude.

At points equidistant from the two vibrators, i.e., along the perpendicular bisector of the line joining the vibrators, the waves from both arrive in phase. Both systems of waves tend to move the water up or down at the same time. The amplitude of the waves along this line is double that due to either of the systems of waves. At some other point sufficiently away from the perpendicular bisector, the crest of one system arrives at the same time as the trough of another, and thus the two systems cancel each other. Destructive interference occurs if the distances of the two vibrators from the point differ by $(n + \frac{1}{2})\lambda$, where λ is the wavelength and n is zero or an integer. Constructive interference occurs if the path difference is $n\lambda$.

An important condition for interference is that the two systems of waves be coherent, i.e., that they always have the same phase relation to each other. If the two slits P and Q in Young's experiment were illuminated by waves from two different sources, interference effects would not be observed. The reason is that waves produced by two sources would have no phase relation to each other. When the two slits are illuminated by different parts of the same wave front, they always arrive at any point beyond the slit with a constant difference in phase.

Theory The mathematical expression for a progressive wave is

$$S = a \cos 2\pi\nu \left\{ \left(t - \frac{x}{v} \right) + \alpha \right\} \qquad (1)$$

where S is the magnitude of the electric or magnetic field, also called displacement, at time t and distance x, a is the amplitude, ν the frequency, v the velocity, and α a term denoting the phase. Due to the superposition of two waves, denoted by subscripts 1 and 2.

$$S = S_1 + S_2 = a_1 \cos 2\pi\nu \left\{ \left(t - \frac{x}{v} \right) + \alpha_1 \right\} + a_2 \cos 2\pi\nu \left\{ \left(t - \frac{x}{v} \right) + \alpha_2 \right\} \qquad (2)$$

Both waves have the same frequency and velocity but different amplitudes and phases; x is measured from any arbitrary point. The displacement at $x = 0$ is given by

$$S = A \cos (2\pi\nu t + \alpha) \qquad (3)$$

where A is the amplitude and α the phase of the resulting wave. By expanding the right-hand sides of Eq. (2) with $x = 0$ and Eq. (3), equating coefficients of $\cos 2\pi\nu t$ and $\sin 2\pi\nu t$, squaring and adding, one can see that

$$A^2 = a_1^2 + a_2^2 + 2a_1 a_2 \cos(\alpha_1 - \alpha_2) \qquad (4)$$

As $\cos (\alpha_1 - \alpha_2)$ varies between +1 and −1, A varies between $(a_1 + a_2)$ and $(a_1 - a_2)$. If the amplitudes a_1 and a_2 are both equal to a, the

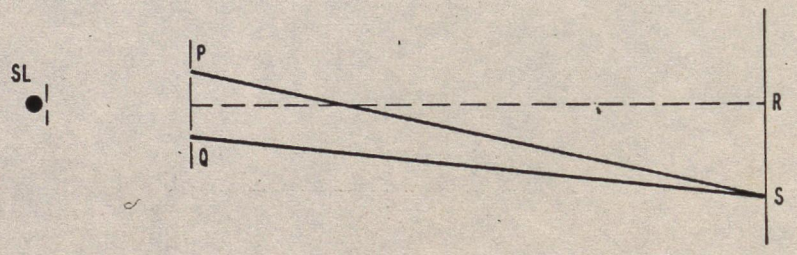

FIG. 1. Young's experiment.

minimum value of A is 0 and the maximum value is $2a$. Since the intensity is proportional to the square of the amplitude, the intensity at the maximum is 4 times that due to either wave. The condition for maximum brightness is: $\alpha_1 - \alpha_2 = 2n\pi$, which corresponds to a path difference of $n\lambda$.

Let R and S, Fig. 1, be the positions of the central fringe and the nth bright fringe below R. Let PQ = s, RS = x, and let D be the distance of the screen from the two slits.

$$PS^2 - QS^2 = \left\{D^2 + \left(x + \frac{s}{2}\right)^2\right\} - \left\{D^2 + \left(x - \frac{s}{2}\right)^2\right\}$$

$$= 2xs$$

$$PS - QS = 2xs/(PS + QS) = 2xs/2D$$

since PS + QS is very nearly equal to $2D$.

$$PS - QS = n\lambda, \text{ therefore } \lambda = \frac{1}{n}\frac{xs}{D} \qquad (5)$$

Equation (5) formed the basis for the first experimental determination of the wavelength of light.

Young's experiment in its original form was difficult to perform and failed to carry conviction when the results were first published. If s = 1 mm, D = 2 meters, the distance between successive fringes for sodium yellow light (λ = 5.89×10^{-5} cm) is only 1.2 mm. The illumination is too poor, the fringes are too close, and two fine slits at 1 mm distance are difficult to produce. The controversy as to whether light is propagated as corpuscles or waves had existed for over a century and a half. Francesco M. Grimaldi, who is regarded as the founder of the wave theory of light, in his book *Physico-Mathesis de Lumine, Coloribus et Iride*, published in 1665, described several experiments on diffraction and interference of light, and presented the rudiments of a wave theory. Newton discussed several diffraction effects in his *Opticks*, published in 1708; he threw his weight heavily on the side of the corpuscular theory of light. Experiments more convincing than those of Young were needed to overthrow a theory based on Newton's authority. Between 1814 and 1816, Fresnel introduced two better methods of producing interference fringes, he also gave a more complete theory of the formation of the fringes, based on the hypothesis of secondary wavelets which was first developed in 1678 by Huygens. Huygens' hypothesis was that every point on a wave front acted as the source for a secondary train of waves and that the envelope of these secondary waves determined every successive position of the wavefront.

The two improved experimental arrangements introduced by Fresnel were the bimirror and the biprism. These solve the difficulty of obtaining two slits sufficiently narrow and close to each other. In the bimirror arrangement, light from a narrow slit is reflected by two plane mirrors inclined at a small angle to each other. Thus the two slits are replaced by the two images of a single slit, and the distance between these can be adjusted by changing the angle between the mirrors. In the biprism arrangement, two small angle prisms joined at their base each produce a small deflection of the light emerging from a single slit, and thus cause two sets of coherent waves to be superposed. A single mirror may also be used as devised by Lloyd to produce interference between wave trains produced by a slit and its image.

Applications of Interference Effects There are many interesting applications of the principle of interference. Refractometers based on interference effects are used to measure small changes in the refractive index of transparent media (see REFRACTION). In the Rayleigh refractometer (see Fig. 2), light from a linear source S, made parallel by a lens L_1, is split into two beams by two fairly wide slits, and then made to pass through two similar tubes T_1 and T_2. After transmission through the tubes, the two beams are brought to a common focus by another lens L_2. If the two tubes contain transparent media of the same refractive index, say the same liquid, the center of the fringe pattern is formed on the axis of the instrument. If the refractive index of the liquid in one of the two tubes is changed, as for example by introducing a solvent, the fringes shift across the focal plane of the viewing lens. By counting the number of fringes which cross a reference line, the equivalent path difference and hence the change in refractive index can be calculated. Compensator plates M_1 and M_2, which restore the fringe pattern to its original position, are convenient devices for counting the fringe shift.

Michelson's method of measuring stellar diameters is another application of interference. A beam mounted over the entrance aperture of

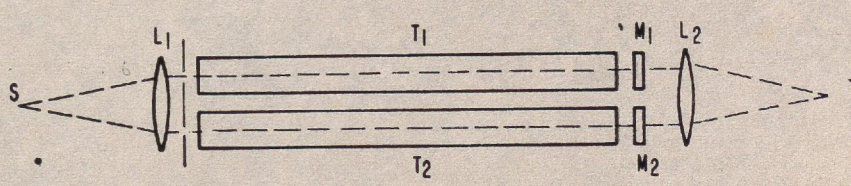

FIG. 2. Rayleigh refractometer.

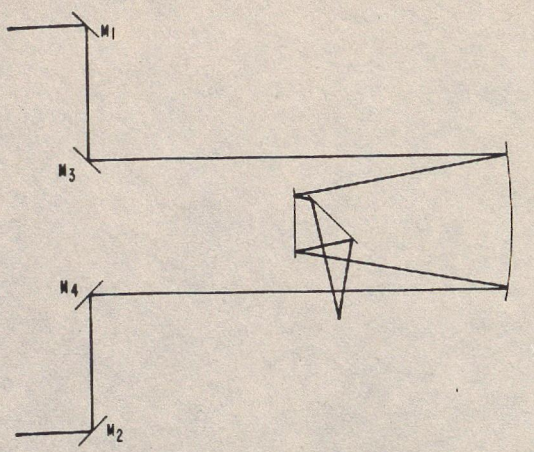

FIG. 3. Stellar interferometer.

a large telescope carries four mirrors as shown in Fig. 3. The arrangement is similar to that of Young's experiment, with the mirrors M_1 and M_2 as the slits and the star as the source. The diffraction image of the star is crossed by interference bands if M_1 and M_2 are relatively close to each other. As the distance between them is increased, the fringes become less distinct and finally disappear. This is due to the fringe pattern from one half of the star being completely canceled by that from the other. If the distance between M_1 and M_2 for disappearance of the fringes is s, r is the distance of the star, d its diameter, and λ the wavelength of light, $d/r = 1.22\lambda/s$. The first star to be measured by this method was Betelgeuse, for which the bands disappeared at $s = 306.5$ cm. Substituting values 5.75×10^{-5} cm for λ, and 1.712×10^{20} cm for r, as determined from the parallax of Betelgeuse, the diameter of the star is found to be 3.918×10^{13} cm, which is 31 per cent greater than the diameter of the earth's orbit around the sun. Several other near stars of large size have since been measured by the same method.

Thin films of transparent media produce striking interference effects, as for example, when a few drops of gasoline are spilled over a wet pavement. The two wave trains which interfere in this case are those reflected from the upper surface of the oil film and from the water-oil interface. The colors of butterflies' wings and sea shells have a similar origin. The so-called Newton's rings are produced by the air film between two partially reflecting, spherical surfaces. The optical quality of a glass surface can be tested by causing interference fringes between it and a standard test plate of high optical quality. The fringes are analogous to contour lines in geographical maps, each new fringe indicating deviation from true flatness by half a wavelength.

Interferometers Interferometers are instruments of high-precision measurement based on the principle of interference. A beam of light is divided into two or more beams by partial reflection and transmission, and these are recombined after they have traveled different path distances. Of the many different types of interferometers, only two which are widely used will be described here, the Michelson interferometer and the Fabry-Perot interferometer.

The Michelson interferometer is shown schematically in Fig. 4. Monochromatic light from

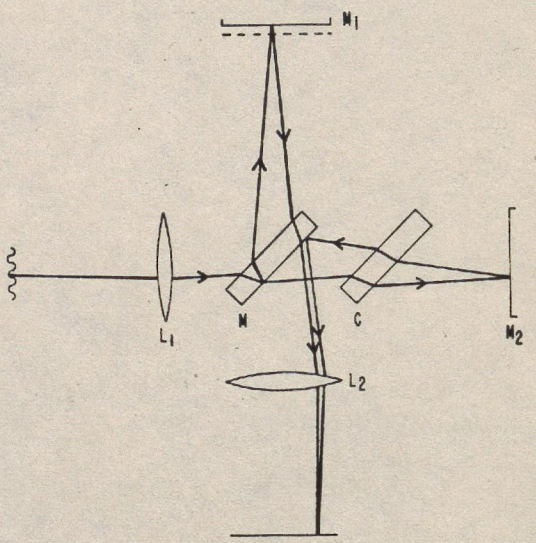

FIG. 4. Michelson interferometer.

an extended source is collimated by a lens L_1 and falls on the beam splitter M of which the hind surface partially reflects half the intensity upward and transmits the other half. The two halves of the beam are returned by the mirrors M_1 and M_2, and the interference pattern is viewed in the focal plane of the lens L_2. C is a compensator plate similar to M, which gives the beam from M_2 an extra path equal to that traveled by the other beam in the beam splitter. The form of the fringes depends on the adjustment of the two mirrors M_1 and M_2. If they are not quite at right angles to each other, and the difference in path of the two beams is small, the image of M_2 in M forms a thin wedge with the front surface of M_1. The fringes are straight and parallel to the apex of the wedge. If the difference in path is large, the two mirrors should be adjusted so that the image of M_2 in M is exactly parallel to M_1. In this case, the fringes are circular. Each circle is due to pencils of light which have a constant inclination to the axis of the lens L_1.

Two of the applications of the Michelson interferometer are of historic importance: the standardization of the meter in terms of the wavelength of light and the Michelson-Morley experiment for the drift of ether. If one of the two mirrors is moved parallel to itself, the pattern of fringes shifts across the field of view.

The displacement of the mirror for each fringe shift is $\lambda/2$. This method was first used by Michelson and Benoit in 1892 for comparing the red line (6438Å) of cadmium with the International Prototype Meter which is kept in Paris, France. More precise measurements of the meter in terms of the wavelength of light have since been made by other observers. Since the wavelength of light is a more reliable standard and can be measured with greater accuracy, it was judged desirable to replace the standard meter by a suitable spectral line as the standard of length. The International Commission of Weights and Measures formally adopted in 1960 the orange-red line of krypton 86 as the standard and defined the meter as exactly 1 650 763.73 wavelengths in vacuum of this line.

The MICHELSON-MORLEY EXPERIMENT of 1887 was an attempt to measure the speed of the ether "wind" past the moving earth. If one arm of the interferometer is in the direction of the earth's motion relative to the ether and the other at right angles to this motion, the relative path difference between the two beams of light is nearly Lv^2/c^2, where L is the length of each arm, v is the velocity of the earth and c is the velocity of light. By floating the interferometer in a pool of mercury and rotating it through 90°, a fringe shift corresponding to twice this path difference should be observed. Accurate experiments showed that the fringes did not shift. This negative result served as the basis for the theory of relativity.

A recent application of the Michelson interferometer is for spectrophotometry of composite sources. The method is especially applicable for the infrared range. One of the two mirrors is moved parallel to itself at a very constant rate. The variation of intensity over a small area at the center of the ring system at P is measured by an infrared detector. If the source were strictly monochromatic, the output signal of the detector would vary sinusoidally with time. The displacement of the mirror between successive maxima is half a wavelength. With a composite source as input, the output is the sum of a large number of sine functions, each of them being due to the energy in a narrow wavelength band of the source. A Fourier transform of the output signal, as may well be obtained with the aid of a digital computer, gives the spectral energy distribution of the source. The compactness of the instrument is a special advantage compared to infrared prism monochromators, and hence several designs of the interferometer spectrophotometer have been developed for use in satellites and space probes. Of special interest is the polarization interferometer. It is used in the short-wavelength region, visible and near IR, where accurate alignment of the moving mirror system is difficult to achieve. The difference in the two indices of refraction of quartz is utilized to produce the path difference between the interfering beams. The incident light is split into two beams with mutually perpendicular planes of polarization, passed through a Soleil prism and then recombined. Change in path difference is produced by sliding one half of the Soleil prism over the other.

The Fabry-Perot interferometer (see Fig. 5) consists of two parallel plates of glass or quartz. The inner surfaces are optically flat and semi-silvered. Light from an extended source is made parallel by a lens L_1, passes through the interferometer and is focused by another lens L_2. A system of circular fringes is observed in the focal plane of L_2. The path of an oblique ray of light in between the two plates is shown in Fig. 5. Interference takes place between the directly transmitted ray and the rays that undergo one or more reflections between the plates. A high degree of wavelength resolution is the main advantage of the Fabry-Perot interferometer. In a typical case of 1-cm separation of plates and 90 per cent reflectance, wavelength resolution is over a million; i.e., two wavelengths 0.005Å apart at 5000Å will give completely distinguishable ring systems. By increasing the reflectance of the plates or the separation between them, the wavelength resolution can be increased to any desired degree. Laser beams which give highly coherent single wavelengths permit plate separation of over a meter. Extensive use has been made of the Fabry-Perot interferometer for precision measurement of wavelengths of spectral lines.

M. P. THEKAEKARA

References

Born, M., and Wolf, E., "Principles of Optics," Chs. 7, 10, and 11, New York, Pergamon Press, 4th edn., 1970.

Cook, A. H., "Interference of Electromagnetic Waves," Oxford, Clarendon Press, 1971.

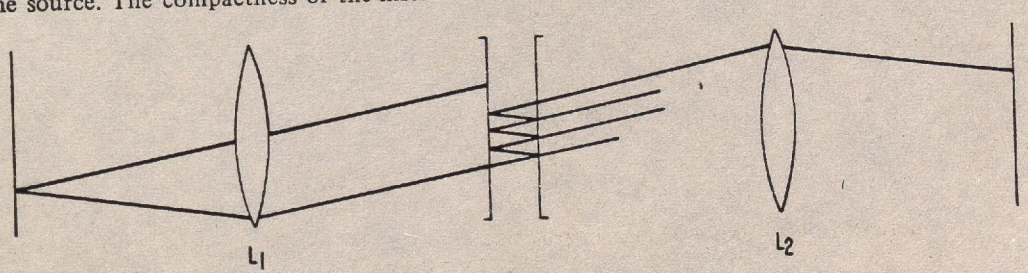

FIG. 5. Fabry-Perot interferometer.

Jenkins, F. A., and White, H. A., "Fundamentals of Optics," Chs. 12, 13, 14, and 17, New York, McGraw-Hill Book Co., 1957.

Klein, M. V., "Optics," Chs. 5 and 6, New York, John Wiley & Sons, Inc., 1970.

Mollet, P., Ed., "Optics in Metrology," Colloquia of the International Commission for Optics, New York, Pergamon Press, 1960. Several excellent articles on applications of interferometry.

Steel, W. H., "Interferometry," London, Cambridge University Press, 1967.

Strong, J., "Concepts of Classical Optics," Chs. 8, 11, 12, and Appendix F, San Francisco, W. H. Freeman and Co., 1958.

Cross-references: COHERENCE, DIFFRACTION BY MATTER AND DIFFRACTION GRATINGS, ELECTROMAGNETIC THEORY, LIGHT, MICHELSON-MORLEY EXPERIMENT, REFRACTION, RELATIVITY, WAVE MOTION.

INTERMOLECULAR FORCES

The terms "intermolecular forces" and "van der Waals forces" refer to the weak forces between molecules, and these forces are to be distinguished from the much stronger interatomic, intramolecular forces of chemical binding. The simplest example of an intermolecular force is provided by the interaction between two noble-gas atoms: The atoms are spherical and the force is central in this case.

Short-range Repulsion The volume of matter in the solid and liquid states is an extensive property, i.e., is proportional to the number of moles or molecules in the specimen, and this implies a molecular "size" or the existence of repulsive forces that prevent two molecules from occupying the same space at the same time. The very low compressibilities of solids and liquids indicate a very strong repulsion of two molecules when they begin to overlap each other. These self-evident conceptions were embodied in the nineteenth-century representation of molecules as little billiard balls. The origin of the "overlap forces" of repulsion was not explained until the advent of quantum mechanics and the Pauli exclusion principle. According to the latter, when two noble-gas atoms begin to overlap, the electrons tend to migrate from the crowded region in the middle to the far ends outside the nuclei, where they exert electrostatic forces that tend to pull the nuclei apart. This effect, which greatly exceeds the direct electrostatic repulsion of the partially shielded nuclei, cannot be represented by any simple analytic potential energy function. For reasons of mathematical convenience, however, an inverse-power law, especially r^{-12}, or a simple exponential function e^{-ar}, where r is the distance between the nuclei of the atoms, is often used to represent the potential energy of the overlap repulsion. The first calculation of an overlap repulsion (between H atoms) was made by Heitler and London in 1927.

Long-range Attraction When two noble-gas atoms are so far apart that there is negligible overlap of their charge clouds or wave packets, the atoms, although neutral and nonpolar, interact through a set of electrostatic multipole terms of which the most important is the lowest-order dipole-dipole term. An instantaneous electric dipole moment in one atom, which averages to zero, induces a dipole moment in the other atom which is proportional to the inducing moment and which interacts with it. It is readily seen that the interaction energy varies as r^{-6}, does not average to zero, and corresponds to an attraction between the atoms. Similarly an instantaneous electric quadrupole moment in one atom induces a dipole moment in the other which interacts with it to give an interaction energy, varying as r^{-8}, which is called the dipole-quadrupole term. These long-range multipole interactions, especially the dipole-dipole term, provide the explanation for the intermolecular attractive forces that are evidenced by imperfect-gas behavior, the Joule-Thomson effect, and the very existence of the liquid state. When the dipole-dipole term is calculated quantum-mechanically, the resulting attractive potential energy, varying as r^{-6}, is called the "dispersion potential." It was first treated by Wang (1927) and then by London (1930).

A Priori Calculations It has long been customary to assume that the intermolecular potential between two neutral, nonpolar molecules consists of a long-range dispersion attraction combined with a short-range overlap repulsion. The combined potential-energy curve for two noble-gas atoms then has a minimum at a distance r_m, and the potential vanishes at a distance σ which is referred to as the slow-collision diameter. However, it is questionable to decompose the interaction potential into parts, and in particular, to use the dispersion potential, which is an asymptotic expression, at distances as small as r_m. The coefficient of the dispersion potential for interactions between pairs of rare-gas atoms has been calculated with great accuracy in recent years, starting from the Schrödinger equation and using a small number of optical data. The a priori calculation of the complete potential energy curve, starting from Schrödinger's equation, is an extraordinarily difficult and laborious procedure even for the simplest atoms and even with the aid of modern electronic computers. Only within recent months (1972) has it been possible to achieve sufficient accuracy to obtain the He–He potential in the neighborhood of its minimum.

Nonadditivity Effects When three or more rare-gas atoms are in proximity, the mutual energy of interaction cannot be expressed as the sum of potential energies for all the interacting pairs, except to a first approximation. The deviations from additivity are associated with many-body forces, and in recent years the three-body interaction has received particular attention. The asymptotic form of the nonad-

of individual electrons must be considered. The inertia of the electrons leads to relaxation effects and to "anomalous skin effect" if the skin thickness becomes smaller than the mean free path of the conduction electrons. In metals that are in the superconducting state, skin effect exists but is affected by the number of superconducting electrons and radiation and absorption processes. An excellent review of these topics is presented in the three-part article by Casimir and Ubbink.[10]

JOHN C. CORBIN, JR.

References

1. Thomson, W., "Mathematical and Physical Papers," Vol. 3, p. 493, Cambridge, Cambridge University Press, 1890.
2. Kennelly, A. E., Laws, F. A., and Pierce, P. H., "Skin Effect in Conductors," *Trans. AIEE*, 34, 1953 (1915).
3. Dwight, H. B., "Skin Effect in Tubular and Flat Conductors," *Trans. AIEE*, 37, 1379 (1918).
4. Ramo, S., and Whinnery, J. R., "Fields and Waves in Modern Radio," Ch. 6, New York, John Wiley & Sons, 1953.
5. McLachlan, N. W., "Bessel Functions for Engineers," Ch. 8, London, Oxford University Press, 1955.
6. Flugge, S., Ed., "Handbuch der Physik," Vol. XVI, "Electric Fields and Waves," p. 182, Berlin, Springer-Verlag, 1958.
7. Moon, P., and Spencer, D. E., "Foundations of Electrodynamics," Ch. 7, New York, Van Nostrand Reinhold, 1960.
8. Simpson, P. G., "Induction Heating," New York, McGraw-Hill Book Co., 1960.
9. Corbin, J. C., "The Influence of Magnetic Hysteresis on Skin Effect," Aerospace Research Laboratories Report 65-167, August 1965 (U.S. Air Force Publication).
10. Casimir, H. B. G. and Ubbink, J., "The Skin Effect; I. Introduction–The Current Distribution for Various Configurations; II. The Skin Effect at High Frequencies; III. The Skin Effect in Superconductors," *Philips Technical Review*, 28, 271–283, 300–315, 366–381 (1967).

Cross-references: ALTERNATING CURRENTS; CONDUCTIVITY, ELECTRICAL; INDUCTANCE; INDUCED ELECTROMOTIVE FORCE.

SOLAR CONSTANT AND SOLAR SPECTRUM

The solar constant is the amount of total solar energy of all wavelengths received per unit time per unit area exposed normally to the sun's rays at the average distance of the earth and in the absence of the earth's atmosphere. The solar spectrum as understood here is the distribution of the same energy as a function of wavelength. The spectrum of the sun extends from x-rays of wavelength 1 Å or below to radio waves of wavelength 100 meters and beyond. Measurements have been made in recent years to cover the entire range. However, for most applications of physics and related fields a more limited range alone need be considered. Ninety-nine per cent of the solar energy is in the range 0.276 μm (1 μm = 10^{-6} m) to 4.96 μm, and 99.9 per cent of the energy is in the range 0.217 μm to 10.94 μm.

The solar irradiance, total and spectral, is important for different branches of physical sciences. The production of solar energy depends on the processes in the interior of the sun. The energy received from the sun yields information about these processes, and about the absorption and reradiation in the intervening space, mainly in the reversing layer of the sun. Comparison of the spectrum outside the earth's atmosphere with that on the ground leads to a knowledge of the absorptive processes in the atmosphere. The sun is an average star, the only one about which detailed knowledge is available at present, and hence the sun's radiation serves as a stepping stone to the science of the stars. Almost all the major topics in geophysics and meteorology, many problems such as heat balance of the earth, physics of the upper atmosphere, fluctuations in the radiation belts, albedo of the earth, and weather forecasting, are closely related to the total and spectral energy received from the sun. There are also many applications in space-age technology. Solar irradiance is the main factor which controls the thermal balance of spacecraft and the output of solar cells. Ultraviolet radiation may degrade spacecraft surfaces or damage insulation materials and optical elements. In some experiments on board satellites, knowledge of the solar irradiance is needed as a standard of calibration for earth-emitted radiation. Spacecraft control systems have to take into account the radiation torques caused by the sun. Thus the solar constant and solar spectrum are standard physical constants which are needed in many areas of physics, astronomy, astrophysics, meteorology, satellite technology, etc.

The energy from the sun has been the topic of research for a long period of time. As is well known, the science of spectroscopy began with Isaac Newton's discovery in 1666 that the white light of the sun is composed of many colors. Infrared was discovered in 1800 when William Herschel probed the dark region beyond the red end of the solar spectrum with a sensitive thermometer. Shortly afterwards followed the discovery of absorption lines in this spectrum by Wollaston in 1802 and by Fraunhofer in 1814. The first known quantitative measurement of the sun's energy was made by Pouillet in 1838. He filled a blackened vessel with water, exposed it to the sun's rays, and measured the rate of rise of temperature. Pouillet determined the value of the solar constant to be 1.7633 calories per square centimeter per minute (1230 W · m^{-2}). This work was continued by several others, notably by K. J. Ångström in

Sweden after whom the Ångström pyrheliometer is named, and by S. P. Langley at the Smithsonian Institution in Washington, D.C. In 1901 Hann's standard work on meteorology quoted without preference three values of the solar constant then currently accepted: Pouillet's, 1.76; Langley's, 3.02; and Ångström's 4.00 $cal \cdot cm^{-2} \cdot min^{-1}$. Following the lead of Pouillet the solar constant is expressed in $cal \cdot cm^{-2} \cdot min^{-1}$ in all of the earlier literature; the preferred unit at present is $W \cdot m^{-2}$. One $cal \cdot cm^{-2} \cdot min^{-1} = 679.3\ W \cdot m^{-2}$.

Work done during this century has helped to narrow down the margin of uncertainty and to map the spectrum more completely and accurately. The most extensive series of measurements were those done by C. G. Abbot and his co-workers of the Smithsonian. This work was begun at the turn of the century and was continued for over 50 years from many different locations around the globe. The basic instrumentation consisted of a spectrobolometer which measures solar spectral irradiance on a relative scale and a water-flow pyrheliometer which measures the total energy on an absolute scale. The readings of the bolometer are made absolute by integrating the area under the curve, adding corrections for the two ends of the spectrum (wavelengths less than 0.346 μm and greater than 2.4 μm) undetected by the bolometer but measured by the pyrheliometer, and equating the total area to that measured by the pyrheliometer. These readings are repeated for different values of air mass and extrapolated to zero air mass by Bouguer's law. Air mass is defined as the ratio of the equivalent path in air of the sun's rays for a given zenith angle to that when sun is at the zenith; it is equal to the secant of the zenith angle if atmospheric refraction effects are ignored. By Bouguer's law the logarithm of the irradiance at any wavelength varies linearly with air mass. The value of the solar constant is obtained by integrating the area under the zero air mass spectrobolometer curve and adding the corrections for the two ends of the spectrum.

The Smithsonian method measures the energy of the whole solar disc. It was adopted by most workers in this field. With the development of high dispersion grating spectrometers and blackbody standards of radiance, a slightly different method was adopted by some observers, notably by M. Nicolet in Belgium and by D. Labs and H. Neckel in Germany. The center of the solar disc is focused on the spectrograph slit, the spectral radiance is measured at many different wavelengths in the continuum between Fraunhofer lines, corrections are made for solar limb darkening and Fraunhofer absorption, spectral data from the Smithsonian and other observers are added for rather wide ranges of wavelength at the two ends of the spectrum, spectral values are extrapolated to zero air mass, and the integral is obtained.

Among values of the solar constant which gained wide acceptance for several years were those proposed by Nicolet in 1951, 1380 $W \cdot m^{-2}$, and by F. S. Johnson in 1954, 1395 $W \cdot m^{-2}$. Both authors had also published detailed solar spectrum curves. Johnson's data were mainly used in the United States and Nicolet's in Europe. The two spectral curves show wide differences, especially in the UV near 0.3 μm where Johnson's values are higher by about 30 per cent and in the IR near 2 μm where Nicolet's values are higher by about 25 per cent. A major difficulty in all ground-based measurements is water-vapor absorption and aerosol scattering. Both of these are large and change considerably in the course of a day, so the extrapolation to zero air mass is open to large uncertainties. In the IR, where the absorption due to water vapor is a major source of error, many authors had assumed the solar spectral curve to be that of a 6000 K blackbody.

In recent years several attempts have been made to measure the solar constant and the solar spectrum from above all or almost all of the atmosphere. The solar constant is determined directly with instruments which measure total irradiance, thus insuring higher accuracy than is possible with the earlier techniques, or integrating spectral irradiance curves extrapolated to zero air mass. A Convair 990 jet aircraft flying at 11.6 km was used by a group of experimenters from NASA's Goddard Space Flight Center (GSFC). At this altitude the instruments are above 80 per cent of the permanent gases and above all of the dust, haze, and smoke of the atmosphere; more importantly, they are above all but 0.1 per cent of the water vapor. Four total irradiance instruments were used: a wire-wound cone radiometer, which measures the incident solar energy in terms of electrical energy required to produce the same change in resistance in the wire; two Ångström pyrheliometers, which measure the solar irradiance on the International Pyrheliometric Scale (IPS 56); and a normal incidence radiometer, which is calibrated with reference to a blackbody. Two types of jet aircraft, Convair 990 and U.S. Air Force B-57B, and the NASA rocket aircraft X-15 served as the observing platforms for several series of measurements made by a joint team of the Eppley Laboratory and the Jet Propulsion Laboratory. The X-15 aircraft reaching an altitude of 85 km provided the first direct measurements of the sun's energy from above the ozone of the atmosphere. The detector was a wire-wound thermopile, calibrated on IPS 56. Measurements from balloons at altitudes 30 km and above were made by research teams of the University of Denver, the University of Leningrad, U.S.S.R., and the Jet Propulsion Laboratory. The detectors were thermopiles calibrated on IPS 56 for the first two and an electrically compensated cavity radiometer for the third. At the ballon altitude the instruments are above all but one per cent of the earth's atmosphere. Another set of data, totally free from atmospheric effects, was obtained by a cavity radiom-

let in 1951, 1380
Johnson in 1954,
s had also published
rves. Johnson's data
United States and
two spectral curves
cially in the UV near
values are higher by
the IR near 2 μm
higher by about 25
v in all ground-based
por absorption and
these are large and
ie course of a day,
ro air mass is open
the IR, where the
por is a major source
d assumed the solar
a 6000 K blackbody.
attempts have been
r constant and the
all or almost all of
nstant is determined
which measure total
her accuracy than is
techniques, or inte-
rves extrapolated to
90 jet aircraft flying
up of experimenters
pace Flight Center
the instruments are
ermanent gases and
, and smoke of the
ntly, they are above
water vapor. Four
s were used: a wire-
which measures the
terms of electrical
the same change in
ngström pyrheliom-
solar irradiance on
etric Scale (IPS 56);
diometer, which is
o a blackbody. Two
ir 990 and U.S. Air
rocket aircraft X-15
latforms for several
ie by a joint team of
d the Jet Propulsion
raft reaching an alti-
first direct measure-
om above the ozone
etector was a wire-
ted on IPS 56. Mea-
at altitudes 30 km
esearch teams of the
University of Lenin-
Propulsion Labora-
ermopiles calibrated
o and an electrically
eter for the third. At
struments are above
earth's atmosphere.
ly free from atmo-
l by a cavity radiom-

eter mounted on the Mars Mariner probe. All of these measurements made at high altitudes and with total irradiance instruments gave converging evidence that the values derived earlier by Nicolet or Johnson from groundbased measurements were too high.

High-altitude solar spectral irradiance data are available mainly from the measurements made on board the Convair 990 at 11.6 km by the NASA GSFC experimenters. The instrumentation consisted of two high-dispersion monochromators, one a Perkin-Elmer, with a lithium fluoride prism for the range 0.3 to 4.0 μm, the other a Zeiss, with a double quartz prism for the range 0.3 to 1.6 μm, a filter radiometer (0.3 to 1.2 μm), a polarization-type interferometer (0.3 to 2.5 μm), and a Michelson-type interferometer (2.6 to 15 μm). These instruments represented some of the best available in precision spectroradiometry. The window material for the aircraft was selected to suit the wavelength range of each instrument, Irtran 4 for the Michelson, sapphire for the Perkin-Elmer and dynasil or infrasil quartz for the other three. Light from the whole solar disc was made to shine on the entrance aperture of each instrument. Corrections for the residual atmosphere above the aircraft were made by applying Bouguer's law. The instruments were calibrated with reference to standards of spectral irradiance, NBS-type lamps for the range below 2.6 μm and high-temperature blackbodies for the longer wavelengths. The Goddard experimenters derived a detailed solar spectral irradiance curve based on these measurements. The area under the curve was found to be almost identical with the value of the solar constant derived from their total irradiance data.

The other highly valuable series of high-altitude spectral measurements are those made by the Eppley-JPL team on board CV 990, B-57B, and X-15 aircraft. The instrument was a 12-channel filter radiometer which gave integrated values of solar irradiance over bandwidths of 500 Å or more. The standard of reference was IPS 56. These results provided a strong confirmation for the Goddard spectral curve.

The value of the solar constant based on all of the high-altitude measurements of recent years is 1353 $W \cdot m^{-2}$. In thermal units the value is 1.940 $cal \cdot cm^{-2} \cdot min^{-1}$. The solar spectral irradiance for zero air mass at the average sun-earth distance is shown in Table 1 and Fig. 1. The probable error in these values is less than 1.5 per cent for the solar constant and less than 5 per cent for spectral irradiance. The solar constant value is 3 per cent lower than the one proposed by Johnson, but very close to the different values proposed in earlier years by C. G. Abbot and his co-workers at the Smithsonian.

These values are the standards recommended by an ad hoc Committee which made a critical evaluation of all available literature on the subject. The committee was sponsored by the NASA Space Vehicles Design Criteria Office and the Institute of Environmental Sciences. They have been proposed as design values by NASA and as engineering standards by IES-ASTM.

Table 1 is an abridged version of more detailed tables published in the original documents.[4,9] These tables cover the wavelength range 50 Å to 6 m and give the spectral irradiance at closer wavelength intervals. The values of E_λ are averages over small bandwidths centered at that wavelength. Bandwidths are 0.01 for $0.3 < \lambda < 0.75$; 0.05 for $0.75 < \lambda < 1.0$; and 0.1 for $\lambda > 1.0$ (all units in μm). This gives the solar spectrum independent of the Fraunhofer

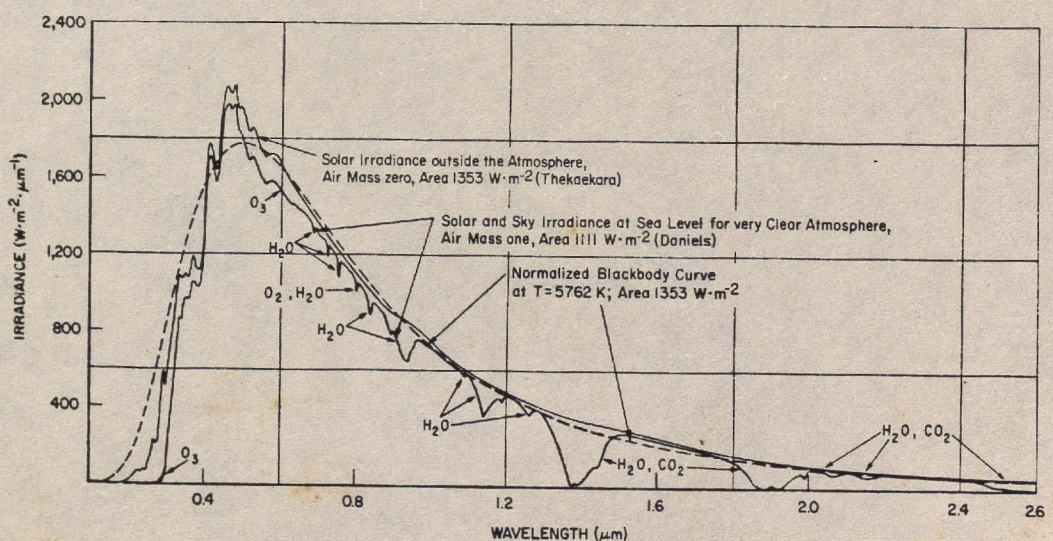

FIG. 1. Solar spectral irradiance outside the earth's atmosphere at 1 A.U. (ASTM standard), normally incident solar irradiance at ground level on very clear days and blackbody spectral irradiance curve at $T = 5762K$.

TABLE 1 SOLAR SPECTRAL IRRADIANCE OUTSIDE THE EARTH'S ATMOSPHERE AT THE MEAN SUN-EARTH DISTANCE (ASTM STANDARD CURVE.)

λ - WAVELENGTH IN μm

E_λ - SOLAR SPECTRAL IRRADIANCE AVERAGED OVER SMALL BANDWIDTH CENTERED AT λ, IN $W \cdot m^{-2} \cdot \mu m^{-1}$

$D_{o-\lambda}$ - PERCENTAGE OF THE SOLAR CONSTANT ASSOCIATED WITH WAVELENGTHS SHORTER THAN λ

SOLAR CONSTANT - 1353 $W \cdot m^{-2}$

λ	E_λ	$D_{o-\lambda}$	λ	E_λ	$D_{o-\lambda}$	λ	E_λ	$D_{o-\lambda}$
0.115	.007	1×10^{-4}	0.43	1639	12.47	0.90	891	63.37
0.14	.03	5×10^{-4}	0.44	1810	13.73	1.00	748	69.49
0.16	.23	6×10^{-4}	0.45	2006	15.14	1.2	485	78.40
0.18	1.25	1.6×10^{-3}	0.46	2066	16.65	1.4	337	84.33
0.20	10.7	8.1×10^{-3}	0.47	2033	18.17	1.6	245	88.61
0.22	57.5	0.05	0.48	2074	19.68	1.8	159	91.59
0.23	66.7	0.10	0.49	1950	21.15	2.0	103	93.49
0.24	63.0	0.14	0.50	1942	22.60	2.2	79	94.83
0.25	70.9	0.19	0.51	1882	24.01	2.4	62	95.86
0.26	130	0.27	0.52	1833	25.38	2.6	48	96.67
0.27	232	0.41	0.53	1842	26.74	2.8	39	97.31
0.28	222	0.56	0.54	1783	28.08	3.0	31	97.83
0.29	482	0.81	0.55	1725	29.38	3.2	22.6	98.22
0.30	514	1.21	0.56	1695	30.65	3.4	16.6	98.50
0.31	689	1.66	0.57	1712	31.91	3.6	13.5	98.72
0.32	830	2.22	0.58	1715	33.18	3.8	11.1	98.91
0.33	1059	2.93	0.59	1700	34.44	4.0	9.5	99.06
0.34	1074	3.72	0.60	1666	35.68	4.5	5.9	99.34
0.35	1093	4.52	0.62	1602	38.10	5.0	3.8	99.51
0.36	1068	5.32	0.64	1544	40.42	6.0	1.8	99.72
0.37	1181	6.15	0.66	1486	42.66	7.0	1.0	99.82
0.38	1120	7.00	0.68	1427	44.81	8.0	.59	99.88
0.39	1098	7.82	0.70	1369	46.88	10.0	.24	99.94
0.40	1429	8.73	0.72	1314	48.86	15.0	4.8×10^{-2}	99.98
0.41	1751	9.92	0.75	1235	51.69	20.0	1.5×10^{-2}	99.99
0.42	1747	11.22	0.80	1109	56.02	50.0	3.9×10^{-4}	100.00

SPHERE AT THE
.)

BANDWIDTH

H WAVELENGTHS

	$D_{0-\lambda}$
91	63.37
48	69.49
85	78.40
37	84.33
45	88.61
59	91.59
03	93.49
79	94.83
52	95.86
38	96.67
09	97.31
1	97.83
2.6	98.22
6.6	98.50
3.5	98.72
1.1	98.91
9.5	99.06
5.9	99.34
3.8	99.51
.8	99.72
.0	99.82
.59	99.88
.24	99.94
10^{-2}	99.98
10^{-2}	99.99
10^{-4}	100.00

structure which different instruments present differently according to their resolution. In the wavelength range 0.3 to 15 μm, which contains nearly 99 per cent of the solar energy, the E_λ values are from the NASA GSFC results, modified slightly for $0.3 < \lambda < 0.7$ in the light of the Eppley-JPL data. At the two extreme ends of the spectrum results from other sources have been used, namely data from experiments on board satellites and rockets for $\lambda < 0.3$ μm [5,6] and compilations of brightness temperature of the sun observed by many different experimenters.[7]

In Fig. 1 are shown two solar spectral curves and a blackbody curve. This figure was prepared by G. Daniels for a NASA monograph of the Space Vehicles Design Criteria series, SP8084, "Surface Atmospheric Extremes." The upper curve gives the solar spectrum outside the atmosphere and is based on the data of Table 1. The lower curve gives the spectrum at sea level on a very clear, dry day (about 2 mm of precipitable water vapor), based on measurements by Daniels. This is the irradiance due to the sun and sky, with the sun at the zenith, and represents about the maximum obtainable at sea level. The annual average H_2O in mid-latitudes is about 19 mm of precipitable water vapor, and hence the absorption bands due to H_2O would be considerably stronger on most days. The dashed line gives a normalized blackbody curve for temperature 5762 K. This is the temperature of the sun as computed from the Stefan-Boltzmann equation, $S = \sigma T^4 r^2 / R^2$, where S is the solar constant 1353 W $\cdot$ m^{-2}; σ is the Stefan-Boltzmann constant, 5.669×10^{-8} W $\cdot$ m^{-2} $\cdot$ deg^{-4}; r is the radius of the solar disc, 6.960×10^8 m; R is the mean sun-earth distance, 1.496×10^{11} m.

The temperature of the sun may also be defined in other ways. From Wien's displacement law, $T\lambda_{max} = C$, the temperature is 6166 K. λ_{max} of the solar spectral curve, which cannot be clearly defined because of Fraunhofer absorption, is taken to be 0.47 μm. The Wien constant is 2.898×10^{-3} m $\cdot$ deg. The effective blackbody temperature of the sun is 5631 K. The effective blackbody temperature is that temperature of the normalized blackbody curve (normalized so that the area under the curve is equal to 1353 W $\cdot$ m^{-2}) for which the area enclosed between the blackbody curve and the solar spectral curve is a minimum. Another definition of the sun's temperature, highly useful in solar physics, is the brightness temperature, which varies with wavelength. It is computed by obtaining the spectral radiance of the sun from the spectral irradiance at one astronomical unit and applying Planck's equation which gives spectral radiance of a blackbody as a function of wavelength and temperature. The brightness temperature of the sun, which is relatively high in the x-ray range, drops to a minimum of about 4540 K at 0.15 μm; it rises to a high value near 6000 K in the visible and near IR; in the IR the temperature falls slowly, reaching a minimum about 4360 K at 50 μm, and then rises to relatively higher values in the microwave region.

The solar constant as stated above is defined for the distance of one astronomical unit (A.U.). The values of solar irradiance when the earth is at the perihelion on January 3 and the aphelion on July 4 are respectively 1399 W $\cdot$ m^{-2} and 1309 W $\cdot$ m^{-2}. The total solar energy received by the earth-atmosphere system per year is 5.45×10^{24} joules or 1.3×10^{24} calories. The irradiance at 1 A.U. leads to an evaluation of the total energy radiated by the sun. The sun radiates energy at the rate of 3.805×10^{26} W. From the relativistic equivalence of mass and energy, the rate of diminution of the mass of the sun is 4.234×10^{12} gm per second. A question might be asked how far this loss of mass in conversion of hydrogen to helium would cause a diminution of solar radiance. The loss is very small compared to the mass of the sun, 1.989×10^{33} gm. If the exponential decay of hydrogen were the only factor, assuming that three-fourths of the sun's mass is hydrogen, it can be shown that the solar radiance would decrease by 0.1 per cent in 8×10^5 years. But other factors such as increased reaction rate due to helium accumulation are involved, and astrophysical theory postulates a secular increase rather than decrease in solar irradiance.

A related question is, what short-term changes, if any, are there in the solar constant and solar spectral irradiance? There are significant changes in the very long wavelength range 6 mm to 6 m with sunspot maxima and minima and with major solar activity.[3] Rocket and satellite experiments in recent years have shown changes also in the x-ray and UV range below 0.3 μm.[5,6] As regards the solar spectrum in the visible and IR and the solar constant, there is a large amount of conflicting experimental data,[1] so it is difficult to state the magnitude of the variations and their relation to sunspot cycles, solar rotation, and other solar phenomena. It would seem that the variations are of the order of one per cent and within the margin of uncertainty in our present knowledge of the solar constant and solar spectrum. With improved techniques in measuring radiant energy, both spectral and total, and better definition of the standard scales of radiometry, it is to be expected that solar energy and its variations will be determined to a considerably higher order of accuracy. This will lead to a better understanding of the sun as a star and its influence on terrestrial phenomena, on weather, in the upper atmosphere, and in oceanography.

MATTHEW P. THEKAEKARA

References

1. Abbot, C. G., "The Sun and the Welfare of Man," Chapter VII, "Solar Variation and Weather," Washington, D.C., Smithsonian Institution, 1929.

2. Abetti, G., "The Sun," London, Faber and Faber, 1955.
3. Allen, C. W., "Astrophysical Quantities," London, The Athlone Press (University of London), 1964.
4. Anon., "Solar Electromagnetic Radiation," NASA Space Vehicles Design Criteria, SP-8005 Revised, NASA, Washington, D.C., 1971.
5. Heath, D. F., "Observations on the Intensity and Variability of the Near Ultraviolet Solar Flux from the Nimbus III Satellite," *J. Atmospheric Sciences*, **26** (5), 1157–1160 (Sept. 1969).
6. Hinteregger, H. E., "The Extreme Ultraviolet Solar Spectrum and Its Variation During a Solar Cycle," *Ann. Géophysique*, **26** (2), 547–554 (1970).
7. Shimabukoro, F. J., and Stacey, J. M., "Brightness Temperature of the Quiet Sun at Centimeter and Millimeter Wavelengths," *Astrophys. J.*, **152** (6), 777–782 (June 1968).
8. Thekaekara, M. P., Kruger, R., and Duncan, C. H., "Solar Irradiance Measurements from a Research Aircraft," *Appl. Optics*, 8 (8), 1713–1732 (Aug. 1969).
9. Thekaekara, M. P., ed., "The Solar Constant and the Solar Spectrum Measured from a Research Aircraft," NASA TR R-351 (Washington, D. C.), Oct. 1970.
10. Thekaekara, M. P., and Drummond, A. J., "Standard Values for the Solar Constant and its Spectral Components," *Nature, Physical Sciences*, **229** (1), 6–9 (Jan. 4, 1971).

Cross-references: METEOROLOGY; INFRARED RADIATION; RADIATION, THERMAL; SOLAR ENERGY SOURCES; SOLAR ENERGY UTILIZATION; SOLAR PHYSICS; SPECTROSCOPY.

SOLAR ENERGY SOURCES*

The existence and persistence of biological life on our planet during the last two or three billion years informs us that the solar light intensity has been very steady for at least that length of time. This in turn points to the fact that the source of solar power must be nuclear energy. Any other source (chemical, gravitational, etc.) would have been exhausted long ago.

The detailed mechanism responsible for solar energy production was identified some thirty years ago. The energy is liberated when, through various networks of reactions, four hydrogen atoms (H) are combined to form one helium atom (He). The difference of mass between the four hydrogen atoms and the helium atom ($\simeq 5 \times 10^{-26}$ gram, corresponding to 26.740 MeV) is then liberated, mostly in the form of gamma rays (about 96 per cent), but also partly in the form of neutrinos (about 4 per cent). The gamma rays (γ) are quickly transformed into heat while the neutrinos (ν) escape immediately and are lost as far as solar heating is concerned.

Some 4.7 billion years ago the mass of gas which was to become the sun was somehow detached from a bigger mass and started to condense under its own weight. From the outside, the stellar mass looked red and was a lot more brilliant than the present sun. The particles composing the gas were mostly hydrogen atoms (about 90 per cent of the atoms), helium (about 9 per cent), then carbon, nitrogen, and oxygen (less than 1 per cent), and finally traces of many other elements including some metals such as iron. As the contraction proceeded the gas grew hotter. When the temperature reached about one million degrees centigrade, thermonuclear reactions between the atoms in the gas started to occur and to liberate nuclear energy. As the power released by these reactions became comparable to the power radiated away by the sun, the contraction stopped, the temperature remained constant and nuclear energy took over the burden of keeping the sun warm. The period of contraction had lasted about 10^7 years. By then the sun had taken its present yellowish appearance and had approximately its present-day brilliance. It had become a so-called main-sequence star.

The transformation of hydrogen into helium then mainly involved the following set of reactions. First in a collision between two hydrogen atoms (^1H) a nuclear reaction takes place and an atom of deuterium (^2H, heavy hydrogen) is formed. This reaction is by far the slowest that we shall meet. It essentially governs the rate of solar energy generation. Next the deuterium reacts with another hydrogen to form an atom of helium 3 (^3He, the light isotope of helium); then two helium 3 thus formed react together to form one helium 4 (^4He) isotope and to release two hydrogen atoms. (The collision between helium 3 and hydrogen yields nothing.) The chain (called the proton-proton or PP I chain) is summarized in Table 1.

TABLE I. THE PROTON-PROTON CHAINS

PP I	$^1H + {}^1H \rightarrow {}^2H + e^+ + \nu$
	$^2H + {}^1H \rightarrow {}^3He + \gamma$
	$^3He + {}^3He \rightarrow {}^4He + 2\,{}^1H$
	or
	$^3He + {}^4He \rightarrow {}^7Be + \gamma$
PP II	$^7Be + e^- \rightarrow {}^7Li + \nu$
	$^7Li + {}^1H \rightarrow {}^8Be + \gamma$
	$^8Be \rightarrow 2\,{}^4He$
	or
	$^7Be + {}^1H \rightarrow {}^8B + \gamma$
PP III	$^8B \rightarrow {}^8Be^* + e^+ + \nu$
	$^8Be^* \rightarrow 2\,{}^4He$
	$^{12}C + {}^1H \rightarrow {}^{13}N + \gamma$
	$^{13}N \rightarrow {}^{13}C + e^+ + \nu$
PP IV	$^{13}C + {}^1H \rightarrow {}^{14}N + \gamma$
	$^{14}N + {}^1H \rightarrow {}^{15}O + \gamma$
	$^{15}O \rightarrow {}^{15}N + e^+ + \nu$
	$^{15}N + {}^1H \rightarrow {}^{12}C + {}^4He$

γ represents gamma rays; ν represents neutrinos

*Editor was unable to locate author. Article is reprinted from first edition.